

Accuracy and precision of an edge-based modulation transfer function measurement method using a variable oversampling ratio

Kenichiro Masaoka; NHK Science & Technology Research Laboratories; Tokyo, Japan

Abstract

The edge-based method standardized in ISO 12233 approximates the modulation transfer function (MTF) one of horizontal or vertical spatial frequency by analyzing a supersampled edge profile obtained from the captured image of a slightly slanted bi-tonal edge. The method describes the slanted projection of pixels sampled on a square grid into a linear array of subpixel-wide bins. An ad hoc correction is available to accommodate the diagonal MTF measurements. However, using a fixed oversampling ratio in the standard method degrades the accuracy and precision of the MTF estimates, owing to misalignment between the projection paths and the bin array. A new edge-based method using a variable oversampling ratio, OMNI-sine, has been proposed to remedy this misalignment. In this study, computer simulations were performed to demonstrate the accuracy and precision of the MTF estimates over a full range of finely sampled slant angles.

Introduction

The modulation transfer function (MTF) is a reliable indicator of the spatial resolution performance of linear and shift-invariant systems. To preserve the convenient transfer-function approach, the MTF is also used for sampled imaging systems, assuming that the object being imaged has spatial frequency components with random phases that are distributed uniformly relative to the sampling sites [1]. In the conventional edge-based method specified by the ISO 12233 standard [2], the spatial frequency response is measured to approximate the MTF as a function of horizontal or vertical spatial frequency. The pixels in a rectangular region of interest (ROI) of a near-vertical or -horizontal bi-tonal edge image are projected parallel to the edge into a horizontal or vertical bin array, respectively, yielding an edge spread function (ESF). The derivative of the ESF yields the line spread function (LSF). The MTF is estimated based on the LSF.

An ad hoc method [3], called “ISO-cosine” in this study, was proposed to accommodate the diagonal MTF measurements as a function of spatial frequency in an orientation perpendicular to the edge by scaling the spatial frequency of the MTF estimate according to the ISO 12233 edge-based method. Recently, the author of this paper proposed a method called “OMNI-sine” to measure the diagonal MTF using a variable oversampling ratio that depends on the slant angle and demonstrated that the method could significantly improve the accuracy and precision of MTF estimates via computer simulation using synthesized edge images [1]. The fundamental difference between the ISO-cosine and OMNI-sine methods lies only in the bin width. Using the OMNI-sine method, the unwanted artifacts of deviations from the original sampling intervals were reduced. However, the slant angles used in the simulation were limited to several critical angles having tangents of simple fractions.

In this study, simulation results are provided on the accuracy and precision of the MTF estimates over a full range of finely

sampled slant angles using the ISO-cosine and OMNI-sine methods, and further possible improvements are discussed.

Methods

In the ISO 12233 edge-based method [2], the pixels sampled on a square grid in the ROI are projected parallel to the edge into a horizontal $1/n_{\text{bin}}$ -pixel-wide bin array, where n_{bin} is the oversampling ratio that is fixed to four. When a vertically oriented rectangular ROI is selected to enclose the near-vertical edge, such that the edge passes through the short sides of the ROI, the slant angle, θ , is measured in a positive clockwise direction from the vertical orientation. Considering the geometric symmetry of the square sampling grid, a symmetric slant angle, θ_{sym} , is defined as the smaller of the two absolute slant angles from the vertical and horizontal orientations ($0^\circ \leq \theta_{\text{sym}} \leq 45^\circ$) [1]. The MTF is underestimated in this method as θ_{sym} increases.

In the ISO-cosine method [3], the MTF as a function of the horizontal or vertical spatial frequency derived by the ISO 12233 edge-based method is corrected by linearly scaling the spatial frequency based on the estimated slant angle to yield the MTF as a function of the spatial frequency in an orientation perpendicular to the edge. This method is equivalent to one that uses a linear bin array perpendicular to the edge orientation with $(\cos \theta_{\text{sym}})/n_{\text{bin}}$ -pixel-wide bins, as shown in Figure 1(a). Note that Eq. 2 in Ref. 3 (for correcting the LSF) should be $\text{LSF}_{\text{corr}}(x) = \text{LSF}(x \sec \theta)$, not $\text{LSF}_{\text{corr}}(x) = \text{LSF}(x \cos \theta)$. The variable oversampling ratio is the inverse of the bin width with $n_{\text{bin}} \sec \theta_{\text{sym}}$.

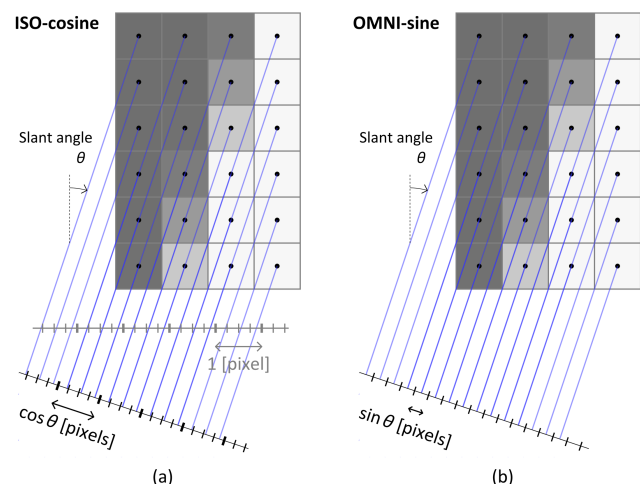


Figure 1. Schematic of binning using the (a) ISO-cosine method and (b) OMNI-sine method when $\tan \theta = 1/3$ and $n_{\text{bin}} = 4$. The blue line segments indicate the projection paths from the pixels on the sampling grid to the positions where they land. The projection paths are aligned with the bin intervals in the OMNI-sine method.

In the OMNI-sine method [1], the bin width is adjusted depending on the slant angle, as shown in Figure 1(b), so that the intervals of each column of the square-grid sampling are aligned with the bin intervals. The bin width is set to $\sin \theta_{\text{sym}}$ multiplied by a power of two, such that the variable oversampling ratio (v_{bin}) approaches n_{bin} , as follows:

$$v_{\text{bin}} = n_{\text{bin}} \cdot 2^{\lceil \log_2(\sin \theta_{\text{sym}}) \rceil - \log_2(\sin \theta_{\text{sym}})}, \quad (1)$$

where $\lceil x \rceil$ rounds x to the nearest integer. For some critical angles, the intervals of each row of the square-grid sample are also aligned with the bin intervals. Figure 2 compares the bin width, $1/v_{\text{bin}}$, used in the OMNI-sine method to that used in the ISO-cosine method, $(\cos \theta_{\text{sym}})/n_{\text{bin}}$, when $n_{\text{bin}} = 4$.

Simulation

To compare the accuracy and precision of the ISO-cosine and OMNI-sine methods, 200×200 -pixel edge images were synthesized analytically for 45,001 slant angles sampled at regular intervals of 0.001° from 0° to 45° in addition to 3,043 critical angles whose tangents were simple fractions having two positive integers ranging from 1 to 100. The virtual camera's MTF was assumed to be $|\text{sinc}(\xi_x, \xi_y)|^3$, which represents a typical MTF of a high-end digital imaging device [4]. The bin array was shifted at a $1/32$ -bin width for each slant angle to obtain 32 MTF estimates using each method. Zero-count bins were scanned from the lower end of the ESF and sequentially interpolated using the average pixel value of the pixels

in the neighboring bin on the lower side of the ESF. The slant angles were set manually in the test simulation to separate the errors in the slant angle estimates from the analysis. More details are provided in Ref. [1].

Results and Discussion

Figure 3 shows the min-max range of the MTF estimates using the ISO-cosine method at the Nyquist and sampling frequencies for the sampled θ_{sym} . It should be noted that the true value of the MTF of $|\text{sinc}(\xi_x, \xi_y)|^3$ depends on the slant angle, which increases slightly as θ_{sym} increases. The errors of the MTF estimates at the sampling frequency are sensitive to slant angles. Around θ_{sym} of a critical angle of $\arctan(1/3)$, the errors are large with many side lobes. Conversely, the errors are small at a critical angle of $\arctan(1/4)$. However, the estimates have larger error peaks as the slant angle is farther away from $\arctan(1/4)$.

Figure 4 shows the MTF estimates using the OMNI-sine method for n_{bin} of 4, 8, and 16. Overall, the errors at the Nyquist frequency for n_{bin} of four have fewer spikes than those of the ISO-cosine method. The errors at the sampling frequency are significantly smaller than those of the ISO-cosine method. The errors for slant angles near 0° , near 45° , and in the vicinity of $\arctan(1/2)$ are large. The larger the n_{bin} , the smaller some existing spikes with more new spikes at some other critical angles. This suggests possible improvements using different n_{bin} depending on the slant angle range. Before considering this possibility, a closer look at the MTF estimates at some critical angles is warranted.

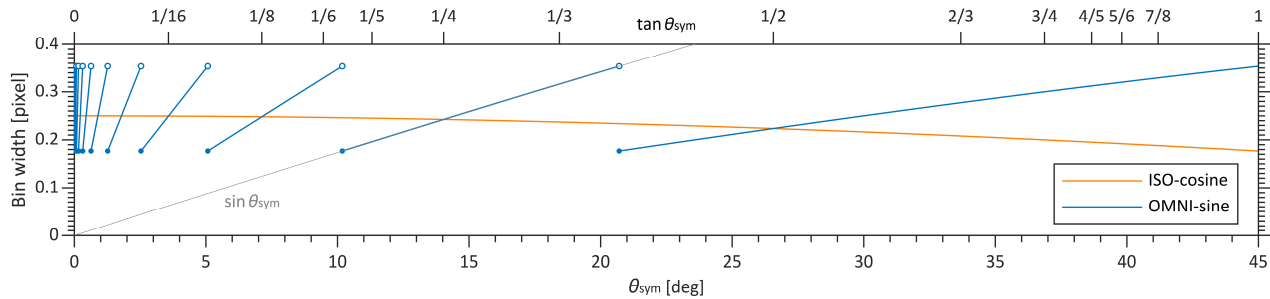


Figure 2. Slant angle vs. variable bin width used in the ISO-cosine and OMNI-sine methods ($n_{\text{bin}} = 4$).

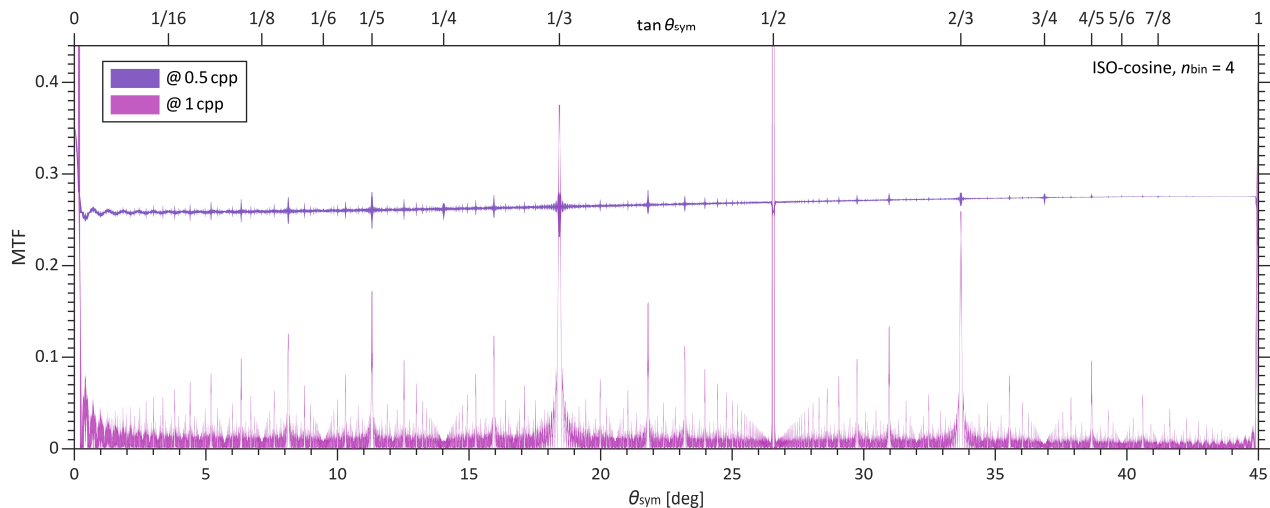


Figure 3. Slant angle vs. MTF estimates at the Nyquist and sampling frequencies using the ISO-cosine method ($n_{\text{bin}} = 4$) for a full range of slant angles of 0 – 45° .

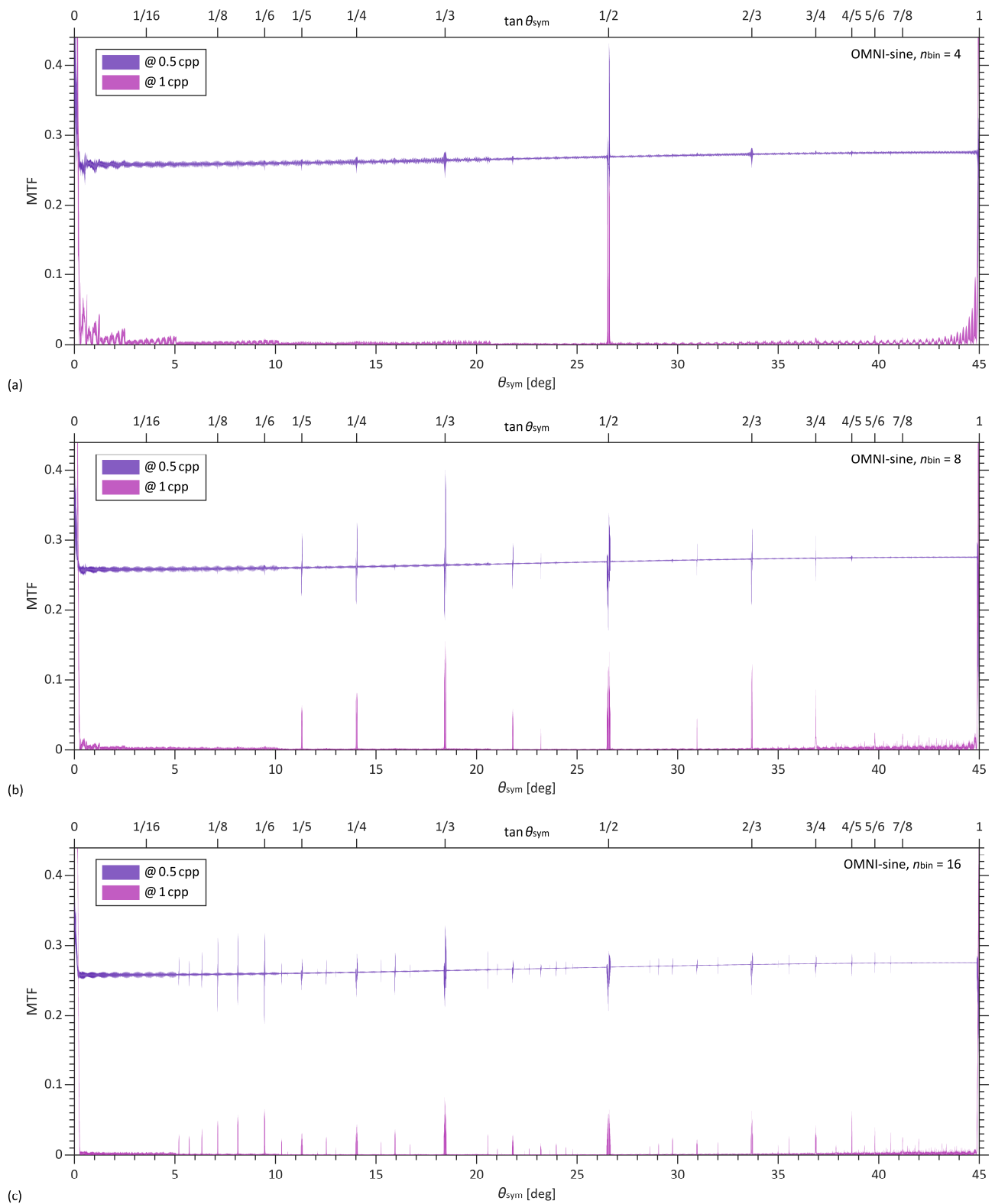


Figure 4. Slant angle vs. MTF estimates at the Nyquist frequency (0.5 cycles/pixel) and sampling frequency (1 cycle/pixel) using the OMNI-sine method with (a) $n_{\text{bin}} = 4$, (b) $n_{\text{bin}} = 8$, and (c) $n_{\text{bin}} = 16$ for a full range of slant angles of 0–45°.

Figure 5 shows the MTF estimates at the Nyquist and sampling frequencies for a range of slant angles of $\arctan(1/3) \pm 0.25^\circ$ for the ISO-cosine and OMNI-sine methods with n_{bin} of four; it compares the MTF curves for the spatial frequencies from 0 to 1 cycle/pixel. The errors of the OMNI-sine method are significantly smaller than those of the ISO-cosine method at the sampling frequency. The errors of the OMNI-sine method with n_{bin} of 8 and 16 (Figures 4(b) and 4(c)) are larger than those of the method with n_{bin} of four

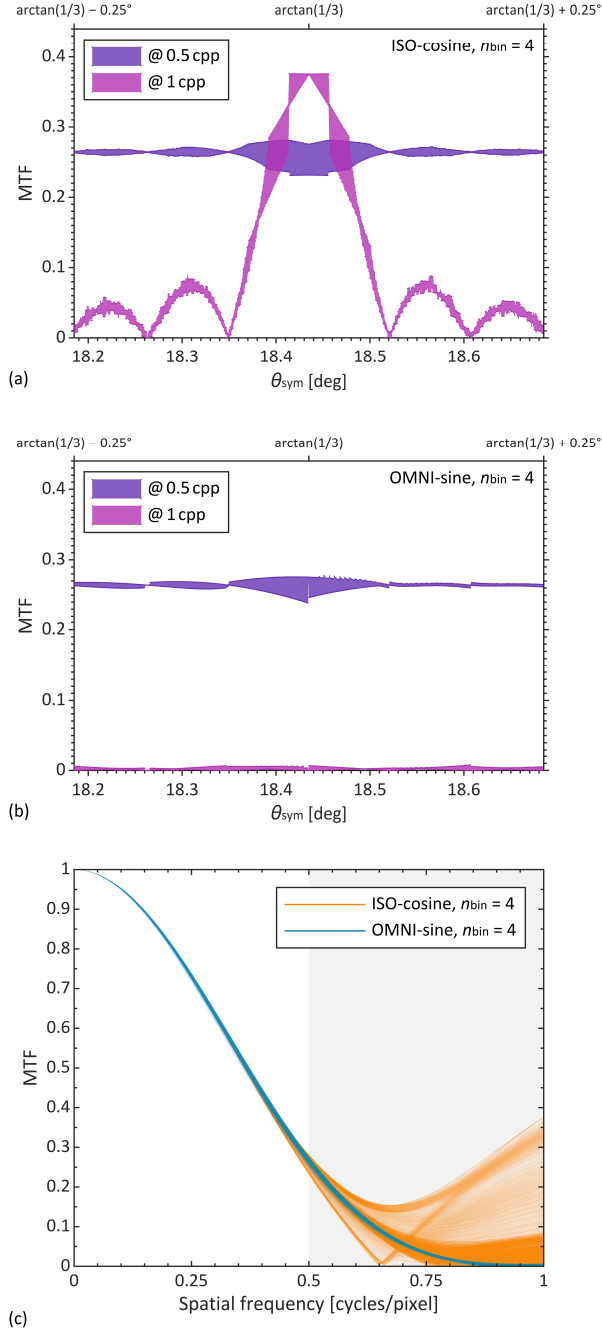


Figure 5. MTF estimates using the ISO-cosine and OMNI-sine methods ($n_{\text{bin}} = 4$) in a range of θ_{sym} of $\arctan(1/3) \pm 0.25^\circ$: MTF estimates at the Nyquist and sampling frequencies using (a) the ISO-cosine method and (b) the OMNI-sine method, and (c) the comparison of their MTF curves between the two methods.

(Figures 4(a) and 5(b)). Notably, there is a small crack in the distribution of the MTF estimation at exactly θ_{sym} of $\arctan(1/3)$ in Figure 5(b).

Figure 6 shows the MTF results of the OMNI-sine method with n_{bin} of 4 and 256 for a range of slant angles of $\arctan(1/2) \pm 0.1^\circ$. In the vicinity of $\arctan(1/2)$, the errors are large and extremely sensitive to the slant angles when n_{bin} is four, indicating the necessity of analysis using finely sampled slant angles.

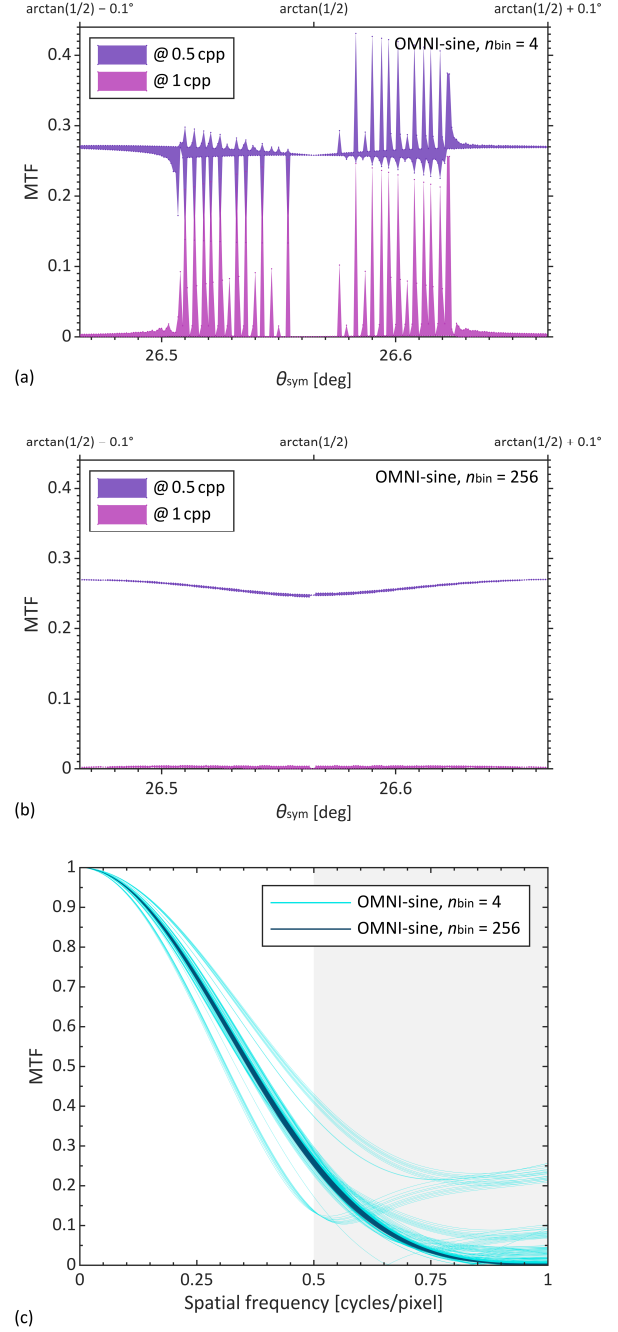


Figure 6. MTF estimates using the OMNI-sine method in a range of θ_{sym} of $\arctan(1/2) \pm 0.1^\circ$: MTF estimates at the Nyquist and sampling frequencies with n_{bin} of (a) four and (b) 256, and (c) comparison of their MTF curves between the n_{bin} values.

To improve the accuracy and precision of the MTF estimation, a patchwork solution is proposed. For slant angles in the range of $\arctan(1/2) \pm 0.075^\circ$, n_{bin} is set to 256. For near- 0° slant angles, n_{bin} is set to eight for $\arcsin(2^{-4.5}) \leq \theta_{\text{sym}} < \arcsin(2^{-3.5})$ and 16 for $0^\circ < \theta_{\text{sym}} < \arcsin(2^{-4.5})$. For near- 45° slant angles, n_{bin} is set to 16 for $43.5^\circ \leq \theta_{\text{sym}} \leq 45^\circ$. For the other slant angle, n_{bin} is set to four. Figure 7 shows the min-max range of the MTF estimation errors using the ISO-cosine and OMNI-sine methods, the errors being obtained by subtracting the true values of the assumed MTF from the MTF estimates at the Nyquist and sampling frequencies for each slant angle. The MTF using the OMNI-sine method can be underestimated by 2–2.5% around critical angles of $\arctan(1/3)$, $\arctan(1/2)$, and $\arctan(2/3)$ at the Nyquist frequency. However, the slant angle ranges are small: within $\pm 0.05^\circ$. Using the OMNI-sine method, the accuracy and precision of the MTF estimates near the sampling frequency are significantly high, which may be useful for evaluating aliasing artifacts as well as estimating the pixel pitch and active pixel size of the image sensor [5]. At the Nyquist frequency, the errors using the ISO-cosine method are slightly larger than those using the OMNI-sine method, owing to the error spikes (Figure 7(a)). Figure 8 compares the MTF estimates for the slant angle range of

$4\text{--}6^\circ$ using the ISO-cosine method (with n_{bin} of four) and the OMNI-sine method with the adjusted n_{bin} . The range was determined by assuming a slant angle of 5° in the ISO standard chart with a possible deviation of $\pm 1^\circ$ in actual measurements. In the ISO-cosine method, the MTF can be overestimated by 8% at the sampling frequency, as confirmed in Figure 3.

The author of this paper performed a computer simulation of MTF estimation using an edge-based method with a fixed-width bin array perpendicular to the edge and found higher accuracy and precision using a small constant bin width, such as $1/32$ pixels, and/or averaging multiple MTF estimates in the different binning phases [6]. However, this not only requires high computational overhead, but the MTF estimation errors are also large at high spatial frequencies. To further improve the accuracy of MTF estimates at critical angles, a method that reconstructs an ESF from samples with irregular spacing using either a local polynomial or kernel-based interpolation was proposed [7]. However, the prerequisite parameter optimization is sophisticated, and further testing of the accuracy and precision of this method is required for a full range of slant angles, including near-critical angles.

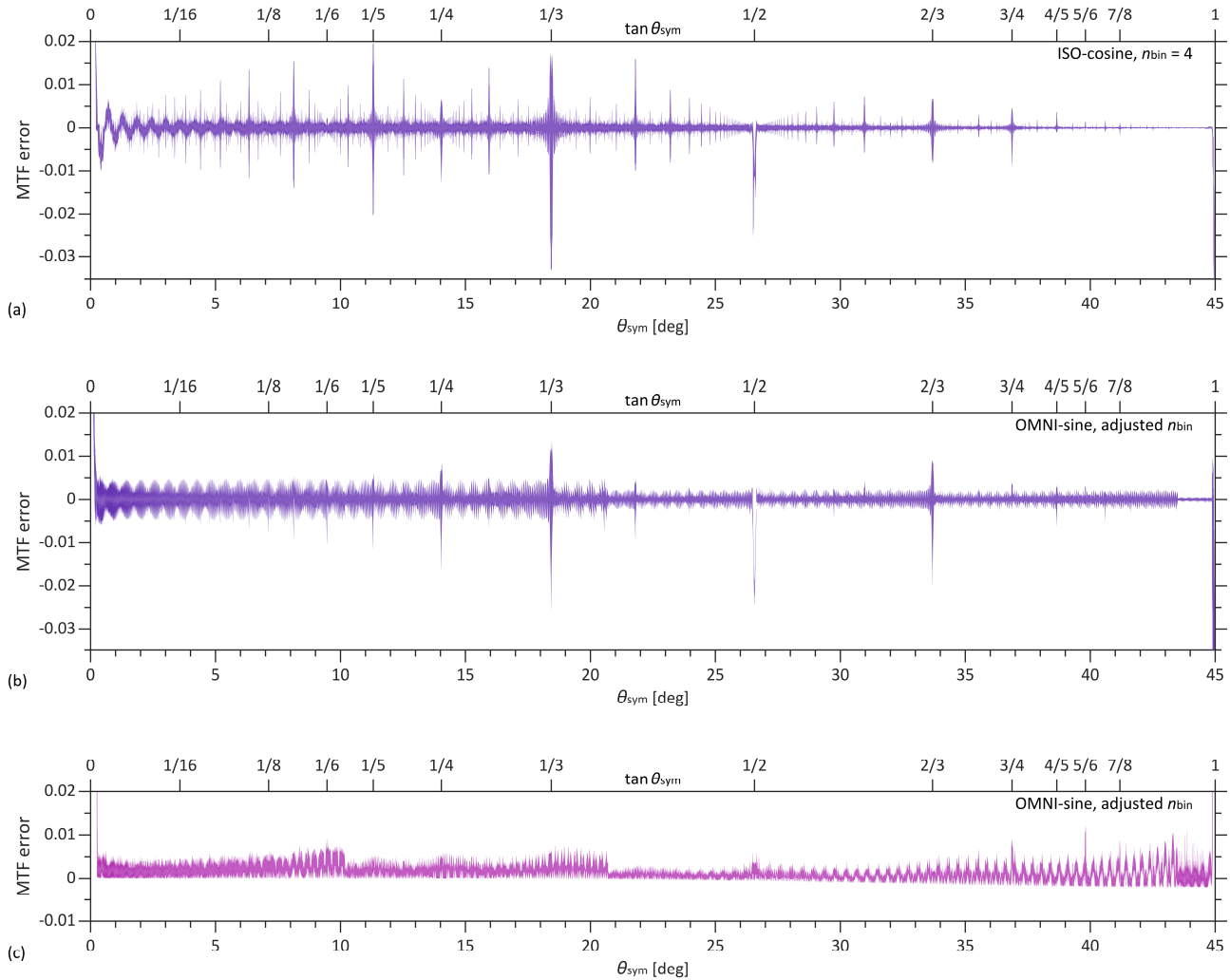


Figure 7. Slant angle vs. MTF error (a) at the Nyquist frequency using the ISO-cosine method and (b, c) at the Nyquist and sampling frequencies, respectively, using the OMNI-sine method with the adjusted n_{bin} .

The OMNI-sine method does not add significant additional computational overhead to real-time MTF measurements, even when multiple ROIs are used. The computational cost of v_{bin} is small, and the value for each ROI is calculated only once at the beginning of each measurement instance because the slant angle is assumed to be constant [8]. The method is effective on actual video camera measurements with image noise because the principle of the proposed method fundamentally alleviates the misalignment of the original pixel intervals on the linear bin array. It is recommended that image noise be reduced by averaging incoming frames to achieve high accuracy and precision.

For diagonal MTF measurements using multiple ROIs, slanted starburst charts are useful [8]. Figure 9(a) shows a four-cycle starburst with a symmetric slant angle of 5° , the diagonal edge having a symmetric slant angle of 40° . The MTF estimates using the ISO-cosine method for this diagonal angle are more accurate than those of the 5° near-vertical and -horizontal edges, based on the results shown in Figure 3. Figure 9(b) shows an eight-cycle starburst with a symmetric slant angle of 3° for the near-vertical and -horizontal edges. Such a smaller slant angle is recommended because the MTF estimates can better approximate the MTF as a function of the exact horizontal and vertical spatial frequencies. The diagonal edges of the symmetric slant angles of 19.5° and 25.5° in the eight-cycle starburst are approximately 1° larger than $\arctan(1/3)$ and 1° smaller than $\arctan(1/2)$, respectively.

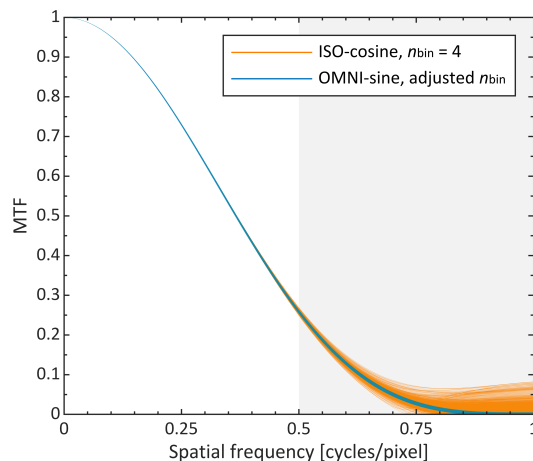


Figure 8. MTF curves estimated using the ISO-cosine and OMNI-sine methods for slant angles of $4\text{--}6^\circ$.

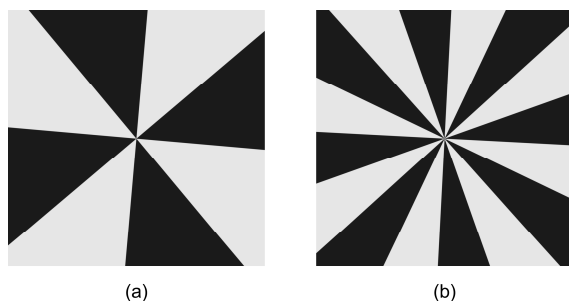


Figure 9. Slanted starburst charts: (a) four cycles with a slant angle of 5° and (b) eight cycles with a slant angle of 3° .

An important area of concern is the shape of the ROI. In the ISO 12233 edge-based method, a rectangular ROI with horizontal and vertical sides is used. In this case, the ROI must be wide enough to enclose a near- 45° edge, and it tends to be small when using an eight-cycle starburst chart so that the ROI will not impinge on the neighboring edges. A rotatable rectangular or trapezoidal ROI is preferable because the ROI can then be placed closer to the center of the starburst chart [8].

Conclusions

This study has demonstrated that the MTF estimates by the OMNI-sine method are more accurate and precise than those by the ISO-cosine method for a full range of finely sampled slant angles, including near-critical angles having tangents of simple fractions. The fundamental difference between the two methods is the bin width, which depends on the slant angle. The OMNI-sine method is easily implementable without impacting the performance of real-time MTF measurements.

References

- [1] K. Masaoka, "Edge-based modulation transfer function measurement method using a variable oversampling ratio," *Opt. Express*, vol. 29, no. 23, pp. 37628–37638, 2021.
- [2] Photography—Electronic Still Picture Imaging—Resolution and Spatial Frequency Responses, ISO 12233:2017.
- [3] J. K. M. Roland, "A study of slanted-edge MTF stability and repeatability," *Proc. SPIE*, vol. 9396, 93960L, 2015.
- [4] N. Koren, 2011 [online], "Understanding image sharpness, part 2: Resolution and MTF curves in scanners and sharpening," <http://www.normankoren.com/tutorials/mtf2.html>.
- [5] T. Battula, T. Georgiev, J. Gille, and S. Goma, "Contrast computation methods for interferometric measurement of sensor modulation transfer function," *J. Electron. Imag.*, vol. 27, no. 1, 013015, 2018.
- [6] K. Masaoka, "Accuracy and precision of edge-based modulation transfer function measurement for sampled imaging systems," *IEEE Access*, vol. 6, no. 1, pp. 41079–41086, 2018.
- [7] F. van den Bergh, "Robust edge-spread function construction methods to counter poor sample spacing uniformity in the slanted-edge method," *J. Opt. Soc. Am. A*, vol. 36, no. 7, pp. 1126–1136, 2019.
- [8] K. Masaoka, K. Arai, and Y. Takiguchi, "Realtime measurement of ultrahigh-definition camera modulation transfer function," *SMPTE Mot. Imag. J.*, vol. 127, no. 10, pp. 14–22, 2018.

Acknowledgements

The author would like to thank Dr. Peter Burns and other eminent experts in the ISO TC42 WG18 for the fruitful discussions.

Author Biography

Kenichiro Masaoka is a principal research engineer at NHK Science and Technology Research Laboratories, Tokyo, Japan. He received his Ph.D. in engineering from the Tokyo Institute of Technology. He worked with Professors Mark Fairchild and Roy Berns for a 6-month residency as a visiting scientist at the Munsell Color Science Laboratory at the Rochester Institute of Technology in 2012. Currently, he is the chair of the Color Metrology Subcommittee and the Spatial Measurements Subcommittee of the International Committee for Display Metrology. He was named a Fellow of the Society for Information Display in 2021.